An Improved Method for Estimating Clumping Index by Digital Hemispheric Photography With Field Measurements

Yidong Tong, Ziti Jiao, Xiaoning Zhang, Siyang Yin, and Jing Guo

***Abstract*— Clumping index (CI) field measurements based on the logarithmic gap fraction averaging (LX) method are widely used. However, some challenges regarding this method have been recognized; e.g., CI overestimation or underestimation occurs in the sampling units where there is no measurement gap, which creates major uncertainties in CI field measurements. To address this issue, we proposed an improved eight-connected LX method that replaces null gap units with the arithmetic mean of the gaps in the eight connected neighboring units, considering the neighboring connections of the natural foliage extension. To validate this method, we designed two controlled experimental schemes based on simulated digital hemispheric photography (DHP) images through the LargE-Scale Remote Sensing Data and Image Simulation Framework (LESS) model considering the leaf area index (LAI) and leaf angle distribution (LAD), respectively, together with collected field measurements. The results showed that our method could almost prevent overestimation and improve underestimated CIs by nearly 20%. In addition, CIs of our method had the smallest error compared to the "true" CIs (error < 0.1). In conclusion, our method can significantly improve the data quality of the simulation results relative to the existing methods and present potentials in the CI measurements of upcoming field campaigns.**

***Index Terms*— Clumping index (CI), digital hemispheric photography (DHP), logarithmic averaging method (LX).**

I. Introduction

CLUMPING index (CI) characterizes the degree of foliage clumping relative to a random distribution in space [1]. The clumping of foliage affects the distribution of solar radiation, thereby affecting canopy photosynthesis and productivity [2], [3]. In addition, CI plays a significant role in ecological processes such as precipitation interception and evapotranspiration [4]. Therefore, CI products have been vital in providing inputs for many land surface models [5].

To properly use CI products, it is critical to conduct enhanced field measurements to provide important data support for validation. Therefore, an accurate and effective measurement method is essential. Indirect methods have been widely used in CI field measurements because of the advantages of high efficiency, low cost, and almost no damage to the canopy [6]. Optical instruments, such as LAI-2200 and digital hemispheric photography (DHP), are commonly used in these methods by measuring the distribution of observed gap fractions. Such methods are generally based on the Beer–Lambert law, which describes the transmission and interception of light radiation by a canopy, as in the following equation [7]:

$$P(\theta) = \mathrm{e}^{-G(\theta)\cdot\frac{\Omega(\theta)\cdot \mathrm{LAI}}{\cos(\theta)}} \tag{1}$$

where $P(\theta)$ is the gap fraction at a zenith angle of θ and $G(\theta)$ is the leaf projection function, which corresponds to the fraction of unit foliage area projected in the direction of θ. LAI is the true leaf area index, and Ω is the CI. The CI has been generally derived via the logarithmic gap fraction averaging method (LX method) based on (1), as in the following equation [8]:

$$\Omega_{\mathrm{LX}}(\theta,\varphi) = \frac{\ln \overline{P(\theta)}}{\ln P(\theta,\varphi)} \tag{2}$$

where $P(\theta)$ is the gap fraction within the finite-length transect at a zenith angle of θ; when there are multiple view zenith angles, the mean value of the gap fraction under each zenith angle should be obtained.

Currently, the LX method based on DHP is widely used in CI field measurements [6], [9], [10]. However, some challenges have been recognized regarding the LX method [11], [12]. Specifically, one assumption of the LX method is that there exist gaps within a finite-length transect. That is, according to (2), $P(\theta)$ is not allowed to be 0 simply because the logarithm of zero is mathematically meaningless. However, the absence of gaps in a finite-length transect within a canopy is inevitable in field measurements, especially in areas with high LAIs where foliage may be densely distributed. Nevertheless, little attention has been devoted to the nongap situation in the original LX method, which has led to possible outliers when utilizing the LX method [11].

Several modifications have been proposed for the case in which no gap exists. At present, there are two commonly used methods: 1) artificially assign one pixel to the nongap unit (one-pixel-gap) before using LX method in (2) [13] or 2) directly ignore the nongap unit (neglection) [14]. Unfortunately, the following issues still exist with both approaches [15], [16]. First, the one-pixel-gap method allocates only one-pixel gap without considering the spatial distribution of

Manuscript received 11 June 2022; revised 16 September 2022; accepted 18 October 2022. Date of publication 21 October 2022; date of current version 7 November 2022. This work was supported by the National Natural Science Foundation of China under Grant 42090013 and Grant 41971288. *(Corresponding author: Ziti Jiao.)*

The authors are with the State Key Laboratory of Remote Sensing Science, Beijing Normal University, Beijing 100875, China (e-mail: tongyd@mail.bnu.edu.cn; jiaozt@bnu.edu.cn; xnzhang@bnu.edu.cn; yinsy@mail.bnu.edu.cn; guojing0404@mail.bnu.edu.cn).

[1]https://doi.pangaea.de/10.1594/PANGAEA.939444.

Digital Object Identifier 10.1109/LGRS.2022.3216274

the foliage, which may subjectively intensify the clumping effect of foliage. Moreover, the degree of such intensification of the clumping effect is closely related to the size of the nongap unit and the total number of pixels within the unit. Thus, the one-pixel-gap method is subject to large uncertainties. Second, the neglection method directly ignores the nongap unit in an area that usually has extreme clumping, which may subjectively weaken the clumping effect. Therefore, the results of the above two methods may be significantly different as the nongap units increase, and both may cause large uncertainties for the measured CIs.

To address this issue, we propose an improved eight-connected LX method considering the natural foliage extension and the neighboring characteristics. To validate our method using so-called "true" CIs, we design two controlled experimental schemes based on simulated DHP images through the LargE-Scale Remote Sensing Data and Image Simulation Framework (LESS). We also use the field-measured DHP images for further validation.

II. Materials and Data

Computer-simulated data based on three-dimensional (3-D) radiative transfer models can accurately describe arbitrarily complex scenarios and have a greater advantage in providing referable CIs as "true" values. In addition, simulated data can autonomously and precisely control the experimental variables and exclude some uncertainties, which is desirable for experimental data. Therefore, we utilized the simulated data as a major source to validate this method.

The simulated DHP images are acquired through LESS as a ray tracing-based 3-D radiative transfer model [Fig. 1(a)]. LESS takes full advantage of forward ray tracing techniques for simulating the radiative budget and backward ray tracing for simulating large-scale images, which makes it possible to simulate various remote sensing data in a single model [17].

As further validation, we also use the field-measured data, which referred to Fang's studies. This measurement was conducted in a farmland near Hailun city in Heilongjiang Province in northeast China. Concurrent destructive LAI measurements along with optical instruments such as DHP were conducted. All of the data associated with Fang's research were published on the PANGAEA website, where more descriptions and details of measurements can be found. Maize and soybean are the two dominant crops in the study area [7], and two maize plots were chosen for our CI validation [Fig. 1(b)].

Fig. 1. (a) Simulated data and (b) field measured data are shown as typical examples.

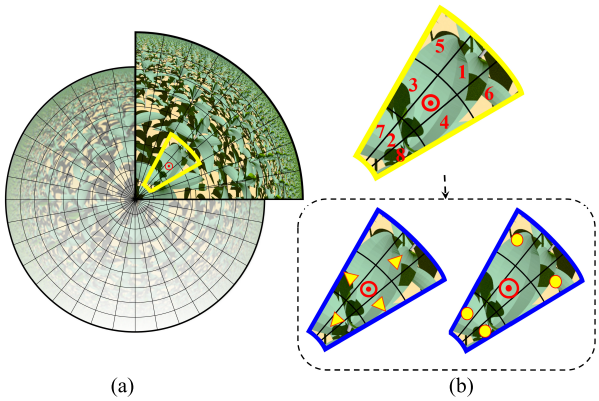

Fig. 2. Process of the eight-connected LX method. (a) Simulated DHP image, and we take the yellow area as an example. (b) Specific procedure. The DHP images are divided with a fixed-angle resolution, i.e., both the azimuth and azimuth intervals are set to 5°.

III. Methodology and Experiments

A. Methodology

As mentioned earlier, the nongap unit is the main source of the problem. Based on previous studies, replacing the null gap unit with a reasonable gap value may be a feasible approach [13], [15]. Our method explores a reasonable substitution approach by considering the natural extension and neighboring properties of foliage. We assume that the growth direction of a 2-D blade always follows its axial direction and expands symmetrically to both sides [18]. In other words, foliage connections are supposed to appear among the neighboring units, and the characteristics of adjacent units may be related, which is the basis for seeking reasonable substitutions among the neighbors. Therefore, we jointly trace the connections along the zenith direction and azimuthal direction based on the properties of the DHP images.

First, we take the nongap unit as the center, as marked by the red circle [Fig. 2(b)]. We start by extending one unit on both sides along the azimuth and zenith directions to form a four-connected area (the triangles in the left blue area). Then, we search for the other four diagonal neighboring units that around the central nongap segments, i.e., the units in the four corners (the yellow circles in the blue right area). Eventually, the eight-connected area is formed by the eight units numbered from 1 to 8, which are enclosed by the yellow lines. Then, we replace the null gap in the center by the arithmetic mean of the gap values in the eight neighbors and itself, as in (3), shown at the bottom of the page, where $P^{\text{Center}}_{\text{num}}$ on the right side represents the number of gap pixels in the center unit, which is 0 here, and P^{N}_{num} (N is $1, 2, \ldots, 8$) is the number of

$$P^{\text{Center}}_{\text{num\_ave}} = \frac{P^{1}_{\text{num}} + P^{2}_{\text{num}} + P^{3}_{\text{num}} + P^{4}_{\text{num}} + P^{5}_{\text{num}} + P^{6}_{\text{num}} + P^{7}_{\text{num}} + P^{8}_{\text{num}} + P^{\text{Center}}_{\text{num}}}{9} \tag{3}$$

gap pixels in the unit numbered N. $P^{\text{Center}}_{\text{num\_ave}}$ on the left side represents the substitution number of the gap pixels.

Therefore, the result ($P^{\text{Center}}_{\text{num\_ave}}$) is assumed to be the reasonable gap value for the nongap unit. It is worth noting that the calculation is carried out by the one-pixel-gap method described above if there is still no gap within the eight connected units.

B. Experimental Design

Since the eight-connected method is proposed to solve the issue regarding the nongap situation, the probability of gaps through the canopy should be considered a key variable for validating the method. Studies have shown that within a plant canopy, the probability that a photon passes unintercepted through a distance s can be modeled as [19]

$$P(s) = \mathrm{e}^{-ksL/D} = \mathrm{e}^{-\tau s} \tag{4}$$

where $\tau = kL/D$ and the variable K is the attenuation of a unit LAI (L) contained within a unit of canopy depth (D), which is highly related to the leaf angle distribution (LAD).

The LAI and LAD are the dominant controls of the probability of gaps according to the typical gap probability model above. They are also the only two structural parameters required for the accurate prediction of reflected, transmitted, and absorbed radiation fluxes [20]. Therefore, the LAI and LAD are selected as two independent variables to design two schemes for the simulated data to validate our new method.

We preliminarily focus on crop field measurements since the combination of the DHP and LX methods has recently been widely used for agricultural crops [9], [10]. Therefore, we build a tree-object based on maize and apply it in the following two schemes. The parameters of the tree-object are referenced from the average morphological structures of maize at different growth stages, i.e., a plant height of 120 cm, a foliage length of 45 cm, and a foliage width of 8 cm [21]. As the major inputs to LESS model, we set the sensor type to circular fisheye and the size of the scene to 10 × 10 m. The camera is set to observe downward at 1.8 m from the ground at each sampling point, and nine photographs were captured in each scene. All photographs are stored in JPEG format at a resolution of 2000 × 2000 pixels.

1) Take LAI as the Variable: In the first scheme, a series of DHP images with various LAIs are simulated (i.e., LAI = 0.4, 0.75, 1.1, and 1.45). The LAD is set to the planophile type with 26.76° as the average leaf angle (ALA). At each LAI, we distributed the tree-object randomly in the scene, where nine sampling points were evenly distributed (Fig. 3).

2) Take LAD as the Variable: In the second scheme, a series of DHP images with three typical functions of the LAD (i.e., planophile, plagiophile, and erectophile) are simulated with 26.76°, 45°, and 63.24° ALAs, respectively [22] (Fig. 4). We also distribute the tree-object randomly in the scene. It is worth noting that the position of the tree-object remains constant under different LADs (Fig. 4), which excludes the location effect.

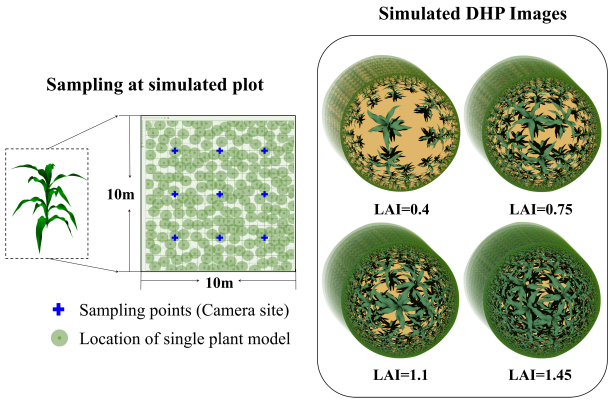

Fig. 3. Scheme (1). (Left) Sampling strategy for the simulated plot. (Right) Simulated DHP images for different LAIs.

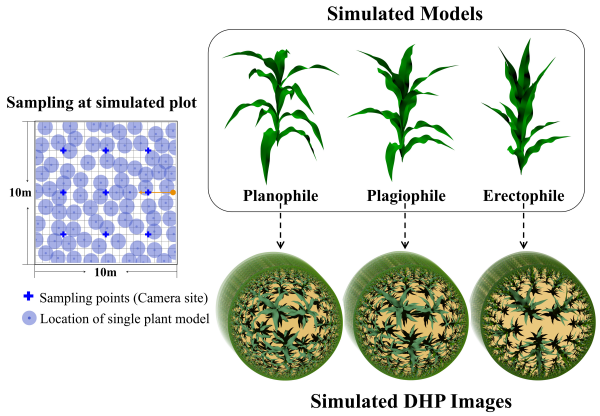

Fig. 4. Scheme (2). (Left) Sampling strategy. (Right) Tree-object with different LADs and the simulated DHP images.

C. Validation

To validate this new method, a cross-comparison of this method was first conducted with other two methods (i.e., the one-pixel-gap method and the neglection method), and then with the "true" CIs.

By definition, the "true" CIs are usually calculated by the ratio between the effective LAI (LAI_{eff}) and the LAI obtained separately in the field measurements as in the following equation [6], [7]:

$$\text{CI} = \frac{\text{LAI}_{\text{eff}}(\text{Optical})}{\text{LAI}(\text{Destructive})}. \tag{5}$$

Regarding the simulated experiments, we obtain the LAI of the whole scene through a tool of LESS, and for LAI_{eff}, we use the formula of Miller [23]

$$\text{LAI}_{\text{eff}} = 2\int_0^{\frac{\pi}{2}} \kappa(\theta)\sin\theta d\theta \tag{6}$$

where k is the mean number of contacts per unit of canopy height and is defined as [24]

$$\kappa(\theta) = \cos\theta \ln[1/P(\theta)] \tag{7}$$

where P is the gap probability at a zenith angle of θ.

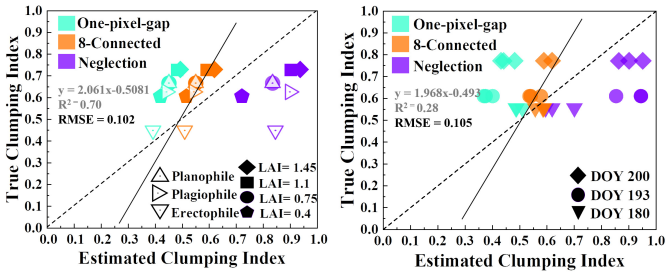

Fig. 5. Scatterplot comparison of the estimated CI and "true" CI of both (a) simulated results and (b) field measured results. (For interpretation of the references to color in this figure, the reader is referred to the web version of this letter.)

Then, we can estimate $\mathrm{LAI}_{\mathrm{eff}}$ by integrating the entire hemispherical gap observations by substituting (7) into (6) [6]

$$\mathrm{LAI}_{\mathrm{eff}} = -2\int_0^{\frac{\pi}{2}} \ln P(\theta)\cos\theta\sin\theta d\theta. \tag{8}$$

To acquire the field dataset, both the destructive and indirect measurements were conducted at seven-day intervals over the entire growing season of maize (DOY 169–262). Considering the potential uncertainties of field measurements due to the stems, senescent leaves, and LAD [7], the anomalies of the measured data since DOY 205 were removed. Finally, the destructive LAI and the $\mathrm{LAI}_{\mathrm{eff}}$ from the optical instruments on DOY 180, 193, and 200 were collected to calculate the "true" CIs using (5).

IV. Results

A. Simulated Experiments

CIs estimated from the three methods show significant differences (Fig. 5) and the results of this proposed method show a significant improvement. The CIs derived by this proposed method are closer to the "true" CIs [$R^2 = 0.70$ and RMSE = 0.102, Fig. 5(a)] than other two methods. Although CIs estimated from the one-pixel-gap method have a relatively high correlation coefficient, its large deviation values from "true" CIs (RMSE = 0.198) explain a prominent underestimation. The neglection method presents the worst result with a low correlation coefficient and a large deviation value with the "true" CIs ($R^2 = 0.16$ and RMSE = 0.235) among these three methods.

For each value of LAI, CIs of the three methods are all ordered as neglection > eight-connected > one-pixel-gap. Compared to the "true" CIs, according to Table I, CIs of the one-pixel-gap method deviate the most with a mean error of 0.22, while CIs of our method are the closest with a mean error of 0.11. In general, our method effectively prevents the overestimation of CIs while reducing the underestimation of CIs from 32% to 16% in scheme (1).

For different LAD conditions, CIs of the three methods are also ordered as neglection > eight-connected > one-pixel-gap. Our method also performs the best only with an error of 0.08. In general, the eight-connected method reduces the underestimation of CIs from 24% to 5% in (2). Furthermore, the performance of our method differs for various LADs. CIs of the planophile plants deviate the most from the "true" CIs with a mean error of 0.11, whereas CIs of the erectophile plants are the closest to the "true" CIs with a mean error of 0.06. This difference indicates that the LAD affects the eight-connected method. Overall, our method outperforms the competing approaches under various LAD functions.

TABLE I
Results of the Two Schemes

Experimental Design			Estimated CIs				"True" CIs
Varibales		ALA (°)	Neglection	One-Pixel	8-Connected	STDEV	$L_{eff\_Miller}/LAI_{LESS}$
LAI	0.40	26.76	0.72 (+0.12)	0.42 (-0.18)	0.52 (-0.08)	0.15	0.6
	0.75		0.84 (+0.17)	0.45 (-0.21)	0.55 (-0.11)	0.2	0.67
	1.10		0.90 (+0.17)	0.48 (-0.24)	0.59 (-0.14)	0.22	0.73
	1.45		0.94 (+0.21)	0.50 (-0.23)	0.62 (-0.11)	0.23	0.73
LAD	Planophile	26.76	0.84 (+0.17)	0.45 (-0.21)	0.55 (-0.11)	0.2	0.66
	Plagiophile	45	0.90 (+0.28)	0.44 (-0.18)	0.54 (-0.08)	0.24	0.62
	Erectophile	63.24	0.85 (+0.40)	0.39 (-0.05)	0.51 (+0.06)	0.24	0.45

*The values in the brackets are the discrepancies between CIs of the three methods and the "true" CIs.

The results of the three methods (ordered as neglection > eight-connected > one pixel) are not unexpected. As we mentioned before, the area with strong clumping is abandoned by the neglection method, leading to an underestimation of the clumping effect, i.e., higher CIs. Similarly, the area with strong clumping is added to a single gap, thus overestimating the clumping effect, i.e., lower CIs. In contrast, the eight-connected method adopts the arithmetic mean value, reducing the pseudohigh and pseudolow clumping effects. Thus, CIs of the eight-connected method lie between CIs of the other two methods, which is theoretically reasonable.

B. Field Measurement

The results obtained with field measured data are in good agreement with the simulated experiments, and the variation trend of the three methods conforms to the theoretical analysis. CIs estimated from all three methods were comparable to the "true" CIs on DOY 180, with a mean error of approximately 0.05. As maize grew, the foliage density gradually increased, and the probability of nongap increased, which causes a significant difference among the three methods. The mean error of this proposed method just approximates 0.1, while those of the other two methods are greater than 0.3 from DOY 193 to 205. The validation confirms the simulation results above, providing further evidences that the proposed method presents a significant improvement for estimating CI by the DHP technique with field measurements.

V. Discussion and Conclusion

This letter explores an improved method to address the challenge of applying the LX method to CI field measurements. The new method is based on the experience of previous studies and considers the continuity of foliage growth, applying a reasonable substitution to solve the nongap case.

In conclusion, our new method significantly improves the LX method in comparison with the previously developed methods. For the simulated experiments, our method can

almost prevent overestimation and improve underestimated CIs by nearly 20%. Furthermore, CIs of our method are the closest to the "true" CIs (error < 0.1) under various LAIs and LADs being explored. For the field measurement, our method exhibits similar trends with the simulation results.

Nevertheless, some challenges regarding the uncertainties inevitably exist in CI field measurement. First, downward DHP images are difficult to distinguish between shaded leaves and soil, especially in a sunny day [25]. Second, different angular intervals in Fig. 2 may yield different CI estimates [6], and may lead to some uncertainties for this proposed method, which deserves further efforts in future. Third, the data used in this study are mainly based on simulated DHP images considering the feasibility of acquiring "true" CI value, although some field measurements are attempted in this study. Thus, the accuracy of our new method remains to be further explored for more field measurements in the near future. In addition, we concentrate on the application of the LX method with crops. However, we believe that this improved method is simple and efficient and has potential for other plant types.

Despite its preliminary characteristics, this study clearly indicates that our new method effectively improves upon the overestimation and underestimation problems of previous methods. The results show that our method is more reliable under various LAIs and LAD functions for a cropland canopy. In general, the developed method improves the data quality of CI measurements to a great extent and thus exhibits potential for the validation of CI products.

REFERENCES

[1] J. Pisek et al., "Intercomparison of clumping index estimates from POLDER, MODIS, and MISR satellite data over reference sites," *ISPRS J. Photogramm. Remote Sens.*, vol. 101, pp. 47–56, Mar. 2015, doi: 10.1016/j.isprsjprs.2014.11.004.

[2] J. M. Chen, C. H. Menges, and S. G. Leblanc, "Global mapping of foliage clumping index using multi-angular satellite data," *Remote Sens. Environ.*, vol. 97, pp. 447–457, Sep. 2005, doi: 10.1016/j.rse.2005.05.003.

[3] J. M. Chen, J. Liu, S. G. Leblanc, R. Lacaze, and J.-L. Roujean, "Multi-angular optical remote sensing for assessing vegetation structure and carbon absorption," *Remote Sens. Environ.*, vol. 84, no. 4, pp. 516–525, Apr. 2003, doi: 10.1016/S0034-4257(02)00150-5.

[4] S. Wei and H. Fang, "Estimation of canopy clumping index from MISR and MODIS sensors using the normalized difference hotspot and darkspot (NDHD) method: The influence of BRDF models and solar zenith angle," *Remote Sens. Environ.*, vol. 187, pp. 476–491, Dec. 2016, doi: 10.1016/j.rse.2016.10.039.

[5] J. M. Chen et al., "Effects of foliage clumping on the estimation of global terrestrial gross primary productivity," *Global Biogeochem. Cycles*, vol. 26, no. 1, pp. 1–18, 2012, doi: 10.1029/2010GB003996.

[6] H. Fang, "Canopy clumping index (CI): A review of methods, characteristics, and applications," *Agricult. Forest Meteorol.*, vol. 303, Jun. 2021, Art. no. 108374, doi: 10.1016/j.agrformet.2021.108374.

[7] T. Nilson, "A theoretical analysis of the frequency of gaps in plant stands," *Agricult. Meteorol.*, vol. 8, pp. 25–38, May 1971, doi: 10.1016/0002-1571(71)90092-6.

[8] A. R. G. Lang and X. Yueqin, "Estimation of leaf area index from transmission of direct sunlight in discontinuous canopies," *Agricult. Forest Meteorol.*, vol. 37, no. 3, pp. 229–243, 1986, doi: 10.1016/0168-1923(86)90033-X.

[9] H. Fang, Y. Ye, W. Liu, S. Wei, and L. Ma, "Continuous estimation of canopy leaf area index (LAI) and clumping index over broadleaf crop fields: An investigation of the PASTIS-57 instrument and smartphone applications," *Agricult. Forest Meteorol.*, vols. 253–254, pp. 48–61, May 2018, doi: 10.1016/j.agrformet.2018.02.003.

[10] Y. Ryu et al., "How to quantify tree leaf area index in an open savanna ecosystem: A multi-instrument and multi-model approach," *Agricult. Forest Meteorol.*, vol. 150, no. 1, pp. 63–76, Jan. 2010, doi: 10.1016/j.agrformet.2009.08.007.

[11] J. M. Chen and T. A. Black, "Foliage area and architecture of plant canopies from sunfleck size distributions," *Agricult. Forest Meteorol.*, vol. 60, no. 3, pp. 249–266, Aug. 1992, doi: 10.1016/0168-1923(92)90040-B.

[12] K. R. Whitford, I. J. Colquhoun, A. R. G. Lang, and B. M. Harper, "Measuring leaf area index in a sparse eucalypt forest: A comparison of estimates from direct measurement, hemispherical photography, sunlight transmittance and allometric regression," *Agricult. Forest Meteorol.*, vol. 74, no. 3, pp. 237–249, May 1995, doi: 10.1016/0168-1923(94)02189-Q.

[13] P. R. van Gardingen, G. E. Jackson, S. Hernandez-Daumas, G. Russell, and L. Sharp, "Leaf area index estimates obtained for clumped canopies using hemispherical photography," *Agricult. Forest Meteorol.*, vol. 94, no. 3, pp. 243–257, May 1999, doi: 10.1016/S0168-1923(99)00018-0.

[14] J.-M.-N. Walter, R. A. Fournier, K. Soudani, and E. Meyer, "Integrating clumping effects in forest canopy structure: An assessment through hemispherical photographs," *Can. J. Remote Sens.*, vol. 29, no. 3, pp. 388–410, Jan. 2003.

[15] A. Gonsamo, J.-M.-N. Walter, and P. Pellikka, "Sampling gap fraction and size for estimating leaf area and clumping indices from hemispherical photographs," *Can. J. Forest Res.*, vol. 40, no. 8, pp. 1588–1603, Aug. 2010. Accessed: May 17, 2022. [Online]. Available: https://www.proquest.com/docview/748913690/231CA0557DDE48CEPQ/1

[16] S. G. Leblanc, J. M. Chen, R. Fernandes, D. W. Deering, and A. Conley, "Methodology comparison for canopy structure parameters extraction from digital hemispherical photography in boreal forests," *Agricult. Forest Meteorol.*, vol. 129, nos. 3–4, pp. 187–207, Apr. 2005, doi: 10.1016/j.agrformet.2004.09.006.

[17] J. Qi et al., "LESS: LargE-Scale remote sensing data and image simulation framework over heterogeneous 3D scenes," *Remote Sens. Environ.*, vol. 221, pp. 695–706, Feb. 2019, doi: 10.1016/j.rse.2018.11.036.

[18] A. Runions, M. Fuhrer, B. Lane, P. Federl, A.-G. Rolland-Lagan, and P. Prusinkiewicz, "Modeling and visualization of leaf venation patterns," *ACM Trans. Graph.*, vol. 24, no. 3, p. 702, Jul. 2005, doi: 10.1145/1073204.1073251.

[19] X. Li and A. H. Strahler, "Modeling the gap probability of a discontinuous vegetation canopy," *IEEE Trans. Geosci. Remote Sens.*, vol. GRS-26, no. 2, pp. 161–170, Mar. 1988, doi: 10.1109/36.3017.

[20] X. Zou et al., "Photographic measurement of leaf angles in field crops," *Agricult. Forest Meteorol.*, vol. 184, pp. 137–146, Jan. 2014, doi: 10.1016/j.agrformet.2013.09.010.

[21] M. L. España, F. Baret, F. Aries, M. Chelle, B. Andrieu, and L. Prévot, "Modeling maize canopy 3D architecture: Application to reflectance simulation," *Ecol. Model.*, vol. 122, no. 1, pp. 25–43, Oct. 1999, doi: 10.1016/S0304-3800(99)00070-8.

[22] M. Weiss, F. Baret, G. J. Smith, I. Jonckheere, and P. Coppin, "Review of methods for in situ leaf area index (LAI) determination," *Agricult. Forest Meteorol.*, vol. 121, nos. 1–2, pp. 37–53, Jan. 2004, doi: 10.1016/j.agrformet.2003.08.001.

[23] J. B. Miller, "A formula for average foliage density," *Aust. J. Bot.*, vol. 15, no. 1, pp. 141–144, 1967, doi: 10.1071/bt9670141.

[24] J. M. Chen and T. A. Black, "Measuring leaf area index of plant canopies with branch architecture," *Agricult. Forest Meteorol.*, vol. 57, no. 1, pp. 1–12, Dec. 1991, doi: 10.1016/0168-1923(91)90074-Z.

[25] H. Fang, W. Li, S. Wei, and C. Jiang, "Seasonal variation of leaf area index (LAI) over paddy Rice fields in NE China: Intercomparison of destructive sampling, LAI-2200, digital hemispherical photography (DHP), and AccuPAR methods," *Agricult. Forest Meteorol.*, vols. 198–199, pp. 126–141, Nov./Dec. 2014, doi: 10.1016/j.agrformet.2014.08.005.